

Images are very important in the remainder of this book. They may be formed by the eye, a camera, an x-ray machine, a nuclear medicine camera, magnetic resonance imaging, or ultrasound. The concepts developed in Chap. 11 can be used to understand and describe image quality. The same concepts are also used to reconstruct computed tomographic or magnetic resonance images of the body. A very complete, advanced mathematical treatment of all kinds of images is found in a 1500-page book by Barrett and Myers (2004). A history of medical imaging has been written by Kevles (1997).

The convolution integral of Sect. 12.1 shows how the response of a linear system can be related to the input to the system and the impulse (δ -function) response of the system. It forms the basis for the rest of the chapter. The Fourier-transform properties of the convolution are also described in this section. Section 12.2 introduces quantitative ways to relate the image to the object, using the techniques developed in Chap. 11 to describe the blurring that occurs. Section 12.3 shows the importance of different spatial frequencies in an image and their effect on the quality of the image.

Sections 12.4 and 12.5 pose the fundamental problem of reconstructing slices from projections and introduce two techniques for solving it: the Fourier transform and filtered back projection. Section 12.6 provides a numerical example of filtered back projection for a circularly symmetric object.

This chapter is quite mathematical. The key understanding to take from it is the relationship between spatial frequencies and image quality in Sect. 12.3.

12.1 The Convolution Integral and Its Fourier Transform

12.1.1 One Dimension

We now apply the techniques developed in Chap. 11 to describe the formation of images. An image is a function of

position, usually in two dimensions at an *image plane*. We start with the simpler case of an image extending along a line. Functions of time are easier to think about, so let us imagine a one-dimensional example that is a function of time: a high-fidelity sound system. A hi-fi system is (one hopes) *linear*, which means that the relationship between the output response and a complicated input can be written as a superposition of responses to more elementary input functions. The output might be the instantaneous air pressure at some point in the room; the input might be the air pressure at a microphone or the magnetization on a strip of tape.

It takes a certain amount of time for the signal to propagate through the system. In the simplest case the response at the ear would exactly reproduce the response at the input a very short time earlier. In actual practice the response at time t may depend on the input at a number of earlier times, because of limitations in the electronic equipment or echoes in the room. If the entire system is linear, the output $g(t)$ can be written as a superposition integral, summing the weighted response to inputs at other times. If $f(t')$ is the input and h is the weighting, the output $g(t)$ is

$$g(t) = \int_{-\infty}^{\infty} f(t')h(t, t') dt'. \quad (12.1)$$

Variable t' is a dummy variable. The integration is over all values of t' and it does not appear in the final result, which depends only on the functional forms of f and h . Note also that if f and g are expressed in the same units, then h has the dimensions of s^{-1} .

If input f is a δ function at time t'_0 , then

$$g(t) = \int_{-\infty}^{\infty} \delta(t' - t'_0)h(t, t') dt' = h(t, t'_0). \quad (12.2)$$

We see that $h(t, t')$ is the *impulse response* of the system to an impulse at time t' . If the impulse response of a linear system is known, it is possible to calculate the response to any arbitrary input.

If, in addition to being linear, the system responds to an impulse the same way regardless of when it occurs, the system is said to be *stationary*. In the hi-fi example, this means that no one is adjusting the volume or tone controls. For a stationary system the impulse response depends only on the *time difference* $t - t'$:

$$h(t, t') = h(t - t'), \quad (12.3)$$

and the superposition integral takes the form

$$g(t) = \int_{-\infty}^{\infty} f(t')h(t - t') dt'. \quad (12.4a)$$

This is called the *convolution integral*. It is often abbreviated as

$$g(t) = f(t) \otimes h(t). \quad (12.4b)$$

For the hi-fi system the function $h(t - t')$ is zero for all t' larger (later) than t ; the response does not depend on future inputs. For the images we will be considering shortly, where the variables represent positions in the object and image, h can exist for negative arguments.

We saw an example of the impulse response in Sect. 11.15, where we found that the solution of the differential equation for the system was a step exponential, Eq. 11.84. For that simple linear system we can write

$$h(t - t') = \begin{cases} 0, & t < t' \\ (1/\tau_1)e^{-(t-t')/\tau_1}, & t > t'. \end{cases} \quad (12.5)$$

We have seen superposition integrals before: for one-dimensional diffusion (Eq. 4.73) and for the potential (Eq. 7.21) and magnetic field (Eq. 8.14) outside a cell.

There is an important relationship between the Fourier transforms of the functions appearing in the convolution integral, which was hinted at in Sect. 11.15. If the sine and cosine transforms of function h are denoted by $C_h(\omega)$ and $S_h(\omega)$, with similar notation for f and g , the relationships can be written

$$\begin{aligned} C_g(\omega) &= C_f(\omega)C_h(\omega) - S_f(\omega)S_h(\omega), \\ S_g(\omega) &= C_f(\omega)S_h(\omega) + S_f(\omega)C_h(\omega). \end{aligned} \quad (12.6a)$$

This is called the *convolution theorem*. If we were using complex exponential notation, the Fourier transforms would be related by

$$G(\omega) = F(\omega)H(\omega). \quad (12.6b)$$

The convolution of two functions in time is equivalent to multiplying their Fourier transforms.

Equations 12.6a are similar to the addition formulas for sines and cosines, which are of course used in the derivation. To derive them, we take the Fourier transforms of f and h :

$$f(t') = \frac{1}{2\pi} \int_{-\infty}^{\infty} [C_f(\omega) \cos \omega t' + S_f(\omega) \sin \omega t'] d\omega$$

$$\begin{aligned} h(t - t') &= \frac{1}{2\pi} \int_{-\infty}^{\infty} [C_h(\omega) \cos \omega(t - t') \\ &\quad + S_h(\omega) \sin \omega(t - t')] d\omega. \end{aligned}$$

Then

$$\begin{aligned} g(t) &= \int_{-\infty}^{\infty} f(t')h(t - t') dt' \\ &= \left(\frac{1}{2\pi}\right)^2 \int_{-\infty}^{\infty} dt' \left[\int_{-\infty}^{\infty} d\omega [C_f(\omega) \cos \omega t' + S_f(\omega) \sin \omega t'] \right. \\ &\quad \left. \times \int_{-\infty}^{\infty} d\omega' [C_h(\omega') \cos \omega'(t - t') + S_h(\omega') \sin \omega'(t - t')] \right]. \end{aligned}$$

We can use the trigonometric addition formulas and the fact that $\sin(-\omega't') = -\sin \omega't'$ to rewrite and expand this expression, much as we did in the last chapter. Carrying out the integration over t' first and using the properties of integrals of the δ function gives

$$\begin{aligned} g(t) &= \frac{1}{2\pi} \int_{-\infty}^{\infty} d\omega [C_f(\omega)C_h(\omega) - S_f(\omega)S_h(\omega)] \cos \omega t \\ &\quad + \frac{1}{2\pi} \int_{-\infty}^{\infty} d\omega [C_f(\omega)S_h(\omega) + S_f(\omega)C_h(\omega)] \sin \omega t. \end{aligned}$$

Comparison of this with Eqs. 11.57 proves Eq. 12.6a.

Fourier techniques need not be restricted to frequency and time. The quality and resolution of the image on the retina, an x-ray film, or a photograph are best described in terms of *spatial frequency*. The distance across the image in some direction is x , and a sinusoidal variation in the image would have the form $A(\lambda) \sin(2\pi x/\lambda - \phi)$. The spatial frequency, $1/\lambda$, is the number of cycles per unit length and is expressed in cycles per meter or cycles per millimeter. The *wave number* or *angular wave number* is $k = 2\pi/\lambda$, where λ is the wavelength. We can write the variation as $A(k) \sin(kx - \phi)$.

12.1.2 Two Dimensions

The convolution and Fourier transform in two dimensions are needed to analyze the response of a system that forms a two-dimensional image of a two-dimensional object. The object can be represented by function $f(x', y')$ in the *object plane*. The image is given by a function $g(x, y)$ in the image plane:

$$g(x, y) = \int_{-\infty}^{\infty} \int_{-\infty}^{\infty} f(x', y')h(x, x'; y, y') dx' dy'. \quad (12.7)$$

If the contribution of object point (x', y') to the image at (x, y) depends only on the relative distances $x - x'$ and $y - y'$, then the two-dimensional impulse response is $h(x - x', y - y')$, and the image is obtained by the two-dimensional convolution

$$g(x, y) = \int_{-\infty}^{\infty} \int_{-\infty}^{\infty} f(x', y') h(x - x', y - y') dx' dy' \quad (12.8a)$$

or

$$g(x, y) = f(x, y) \otimes \otimes h(x, y). \quad (12.8b)$$

The Fourier transform in two dimensions is defined by

$$\begin{aligned} f(x, y) &= \left(\frac{1}{2\pi}\right)^2 \int_{-\infty}^{\infty} dk_x \\ &\times \int_{-\infty}^{\infty} dk_y [C(k_x, k_y) \cos(k_x x + k_y y) \\ &+ S(k_x, k_y) \sin(k_x x + k_y y)]. \end{aligned} \quad (12.9a)$$

The coefficients are given by

$$C(k_x, k_y) = \int_{-\infty}^{\infty} dx \int_{-\infty}^{\infty} dy f(x, y) \cos(k_x x + k_y y), \quad (12.9b)$$

$$S(k_x, k_y) = \int_{-\infty}^{\infty} dx \int_{-\infty}^{\infty} dy f(x, y) \sin(k_x x + k_y y). \quad (12.9c)$$

The Fourier transforms of the functions in the convolution are related by equations similar to those for the one-dimensional convolution.

$$\begin{aligned} C_g(k_x, k_y) &= C_f(k_x, k_y) C_h(k_x, k_y) \\ &- S_f(k_x, k_y) S_h(k_x, k_y), \\ S_g(k_x, k_y) &= C_f(k_x, k_y) S_h(k_x, k_y) \\ &+ S_f(k_x, k_y) C_h(k_x, k_y). \end{aligned} \quad (12.10)$$

With complex notation we would define the two-dimensional Fourier transform pair by

$$\begin{aligned} F(k_x, k_y) &= \int_{-\infty}^{\infty} \int_{-\infty}^{\infty} f(x, y) e^{-i(k_x x + k_y y)} dx dy, \\ f(x, y) &= \left(\frac{1}{2\pi}\right)^2 \int_{-\infty}^{\infty} \int_{-\infty}^{\infty} F(k_x, k_y) e^{i(k_x x + k_y y)} dk_x dk_y, \end{aligned} \quad (12.11a)$$

and the convolution theorem would be

$$G(k_x, k_y) = F(k_x, k_y) H(k_x, k_y). \quad (12.11b)$$

12.2 The Relationship Between the Object and the Image

12.2.1 Point Spread Function

Suppose that an object in the $x'y'$ plane is described by a function $L(x', y')$ that varies from place to place on the object. The image is

$$E_{\text{image}}(x, y) = \iint L(x', y') h(x, y; x', y') dx' dy'. \quad (12.12)$$

Function h is called the *point spread function*. The point spread function tells how information from a point source at (x', y') spreads out over the image plane. It receives its name from the following. If we imagine that the object is a point described by $L(x', y') = L\delta(x' - x'_0)\delta(y' - y'_0)$, then integration shows that

$$E_{\text{image}} = h(x, y; x'_0, y'_0).$$

The point spread function has the same functional form as the image from a point source, just as did the impulse response in one dimension.

You can verify that the point spread function for an ideal imaging system with magnification m is

$$h(x, y; x', y') = m^2 \delta(x - mx') \delta(y - my'). \quad (12.13)$$

The δ functions pick out the values $(x' = x/m, y' = y/m)$ in the object plane to contribute to the image at (x, y) . You can make the verification by substituting Eq. 12.13 in Eq. 12.12 and using the properties of the δ function from Eq. 11.64.

This discussion assumes that *intensities* add. This is true when the oscillations of the radiant energy (such as the electric field for light waves) have random phases lasting for a time short compared to the measurement time. Such radiant energy is called *incoherent*.¹

We have already seen that when the impulse response in a one-dimensional system depends on coordinate differences such as $t - t'$ (or $x - x'$ or $x - mx'$), the system is stationary. In this case it is also said to be *space invariant*: changing the position of the object changes the position of the image but not its functional form. Stationarity is easier to obtain in a system such as a hi-fi system than in an imaging system, but we usually assume that it holds in an imaging system as well. For a space-invariant system

$$E_{\text{image}}(x, y) = \iint L(x', y') h(x - mx', y - my') dx' dy'. \quad (12.14)$$

¹ These arguments also work for coherent radiation, where the phases are important, but the point spread function is for the amplitude of the wave instead of the square of the amplitude (intensity). The calculation then gives rise to interference and diffraction effects.

This is a two-dimensional convolution. The convolution theorem is

$$\begin{aligned}
 C_{\text{image}}(k_x, k_y) &= C_{\text{object}}(k_x, k_y)C_h(k_x, k_y) \\
 &\quad - S_{\text{object}}(k_x, k_y)S_h(k_x, k_y), \\
 S_{\text{image}}(k_x, k_y) &= C_{\text{object}}(k_x, k_y)S_h(k_x, k_y) \\
 &\quad + S_{\text{object}}(k_x, k_y)C_h(k_x, k_y).
 \end{aligned}
 \tag{12.15}$$

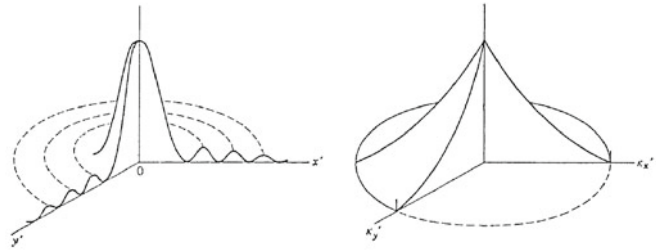


Fig. 12.1 The point spread function and modulation transfer function for a diffraction-limited circular aperture. (Source: Williams and Becklund 1972). Used by permission of the authors

12.2.2 Optical, Modulation, and Phase Transfer Functions

The *optical transfer function* (OTF) is the Fourier transform of the point spread function, $C_h(k_x, k_y)$ and $S_h(k_x, k_y)$. It is analogous to the transfer function for an amplifier (Sect. 11.15). The *modulation transfer function* (MTF) is the amplitude of the OTF:

$$\text{MTF}(k_x, k_y) = \left[C_h^2(k_x, k_y) + S_h^2(k_x, k_y) \right]^{1/2}. \tag{12.16}$$

The *phase transfer function* is

$$\text{PTF}(k_x, k_y) = \tan^{-1} \left(\frac{S_h(k_x, k_y)}{C_h(k_x, k_y)} \right). \tag{12.17}$$

Often the transfer functions are normalized by dividing them by their value at zero spatial frequency.

The modulation transfer function can be measured by using a set of objects for which L varies sinusoidally at different spatial frequencies. The property L cannot be negative and must be offset by a zero-frequency component:

$$L(x, y) = a + b \cos(k_x x + k_y y), \quad 0 < b < a. \tag{12.18}$$

The image is described by

$$\begin{aligned}
 E &= \text{MTF}(0, 0)a \\
 &\quad + \text{MTF}(k_x, k_y)b \cos[k_x x + k_y y + \phi(k_x, k_y)].
 \end{aligned}
 \tag{12.19}$$

The *modulation* of the object is defined to be

$$(\text{modulation}) = \frac{L_{\text{max}} - L_{\text{min}}}{L_{\text{max}} + L_{\text{min}}} = \frac{(a + b) - (a - b)}{(a + b) + (a - b)} = \frac{b}{a}. \tag{12.20}$$

A similar expression defines the modulation of the image. The modulation transfer function is the ratio of the modulation of the image divided by the modulation of the object. The phase of the optical transfer function describes shifts of the phase of the image at each angular frequency along the appropriate axis. It is fully as important as the amplitude, since it describes the evenness or oddness of the image about its stated origin.

The modulation transfer function of an ideal system would be flat for all spatial frequencies. However, there is

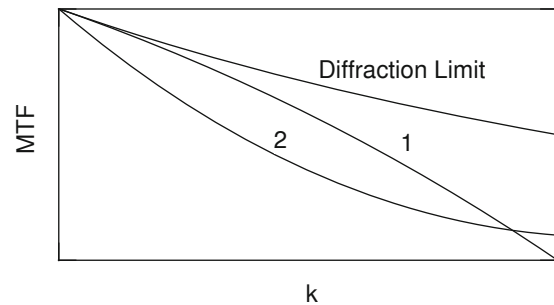


Fig. 12.2 Three possible modulation transfer functions. The *top* one is the diffraction limit for monochromatic light. (Compare it with Fig. 12.1.) Curve 2 is higher than curve 1 at the highest value of k shown, but an image produced by system 2 would not have as much “punch.” It has less content at the middle spatial frequencies

an upper limit imposed by diffraction, if nothing else. Figure 12.1 shows the point spread function and MTF for a diffraction-limited case. Figure 12.2 shows three possible modulation transfer functions for an imaging system. The upper one represents the diffraction limit. It has the same general shape as in Fig. 12.1. Curves 1 and 2 might be for real systems. While the second system transmits more of the highest spatial frequencies, it transmits less of the midrange frequencies, and its image would not have as much “punch” as the first system. Figure 12.3 shows the modulation transfer functions of several photographic films, with (a) being the most sensitive and (e) the least sensitive but with the highest resolution. Photographers are well aware of the trade-off between speed and resolution in film. Fast films are “more grainy” than slow films.

A complex imaging system may have several components, just as the hi-fi system did. If the system is linear, the modulation transfer function for the combined system is the product of the modulation transfer functions for each component. The optical transfer functions combine according to equations like Eq. 12.10.

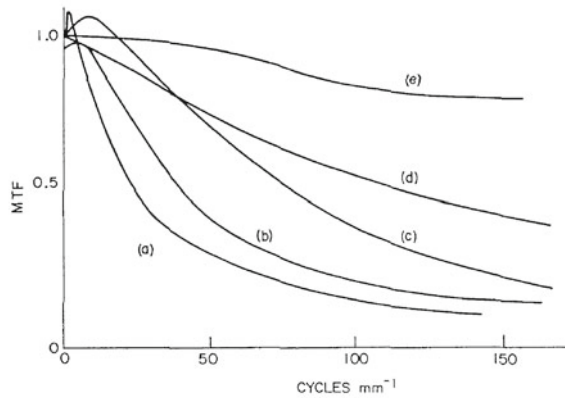


Fig. 12.3 Some representative modulation transfer functions for various photographic films, showing how the resolution decreases as the film sensitivity increases. Film (a) has the greatest sensitivity and worst resolution. Film (e) is the least sensitive (“slowest”) and has the best resolution. (With permission from Shaw 1979)

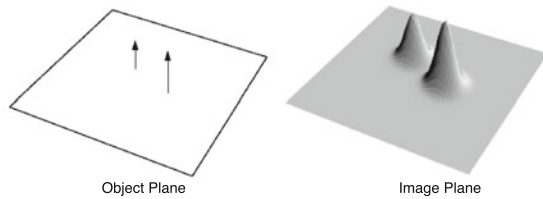


Fig. 12.4 The point spread function. Two impulse sources of different heights are shown in the object plane. The response to them is shown in the image plane

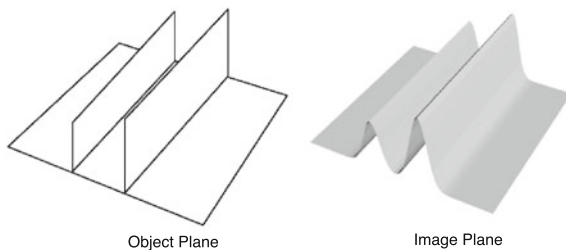


Fig. 12.5 The line spread function. Two line sources are shown in the object plane. The response to them is shown in the image plane

12.2.3 Line and Edge Spread Functions

The *line spread function* is the response of a system to a line object in the object plane. In general, the system is not isotropic and the line spread function depends on the orientation of the line. The Fourier transform of the line spread function along the y axis is $C_h(k_x, 0)$ and $S_h(k_x, 0)$. Figure 12.4 shows a geometrical interpretation of the point spread function. Figure 12.5 shows the line spread function. The *edge spread function* is the response to an object that is a step function. All of these functions are interrelated. A discussion of how one can be obtained from another is found in many places, including Chap. 9 of Gaskill (1978).

12.3 Spatial Frequencies in an Image

There are some universal relationships between the spatial frequencies present in an image and the character of the image. These relationships hold whether the image is a photograph, an x-ray film, a computed tomographic scan, an ultrasound or nuclear medicine image, or a magnetic resonance image. In this section we describe these general relationships, which we will use throughout the rest of the book.

The first general relationship concerns the size of an image and the lowest spatial frequency present. For simplicity, consider the x direction and the corresponding spatial frequencies k . The *object* is nonperiodic. But its *image* is represented by a Fourier series which has period L . We saw in Chap. 11 that if the lowest angular frequency present is ω_0 , the period is $T = 2\pi/\omega_0$. The lowest spatial frequency present (other than zero) is $k_0 = 2\pi/L$. The series has harmonics with separation $\Delta k = k_0$. This leads to the fundamental relationship

$$L = \frac{2\pi}{k_0}. \tag{12.21}$$

The lowest spatial frequency present (which equals the separation of the spatial frequencies) is related to the size of the image L (the “field of view” or FOV).

The second general relationship concerns the spatial resolution in an image and the highest spatial frequency present. If the image has N discrete samples, then the sampling interval or spatial resolution is $\Delta x = L/N$. This allows (or requires) the determination of $N/2$ cosine coefficients and $N/2$ sine coefficients (see Sect. 11.4). The highest spatial frequency present is $k_{\max} = N\Delta k/2$. We obtain

$$\Delta x = \frac{L}{2} \frac{\Delta k}{k_{\max}} = \frac{\pi}{k_{\max}}. \tag{12.22}$$

The spatial resolution is inversely proportional to the highest spatial frequency present. As we saw for the Fourier series representing a square wave, the higher harmonics give fine detail and sharpness to the image.

To reiterate: *The lowest spatial frequency in the image determines the field of view. The lower the minimum spatial frequency, the larger the field of view. The highest spatial frequency in the image determines the resolution. The higher the maximum spatial frequency, the finer the resolution.*

Here are a number of pictures that show how changing the coefficients in certain regions of k space affect an image. Figure 12.6b shows a transverse scan of a head by magnetic resonance imaging. This is a normal image to compare with the following figures. It consists of 256 samples in each direction or 256×256 pixels. The magnitude of its Fourier transform is shown in Fig. 12.6a. Figure 12.7 shows the cosine and sine coefficients in the expansion.

Figures 12.8 and 12.9 show what happens when the high-frequency Fourier components are removed. In the first case

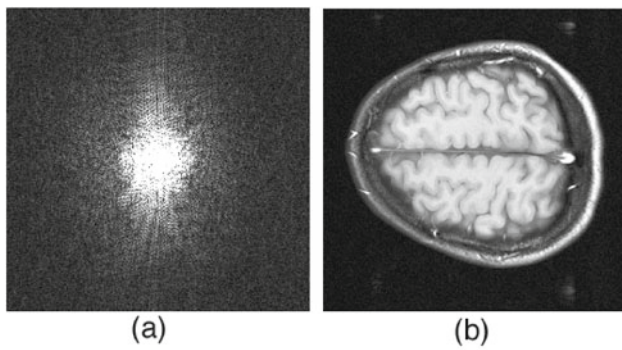


Fig. 12.6 A magnetic resonance imaging head scan: **a** The squared amplitude $C^2 + S^2$ in k space. **b** The image. This is a normal image to compare with the following figures. Prepared by Mr. Tuong Huu Le, Center for Magnetic Resonance Research, University of Minnesota. Thanks also to Prof. Xiaoping Hu

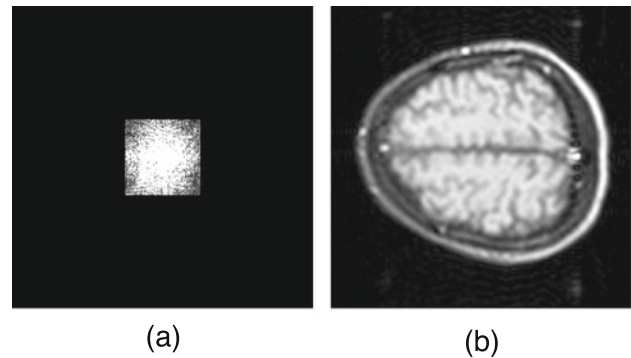


Fig. 12.9 The image that results when the high-frequency Fourier components above $k_{x \max}/4$ and $k_{y \max}/4$ are removed. The blurring is even greater. Prepared by Mr. Tuong Huu Le, Center for Magnetic Resonance Research, University of Minnesota. Thanks also to Prof. Xiaoping Hu

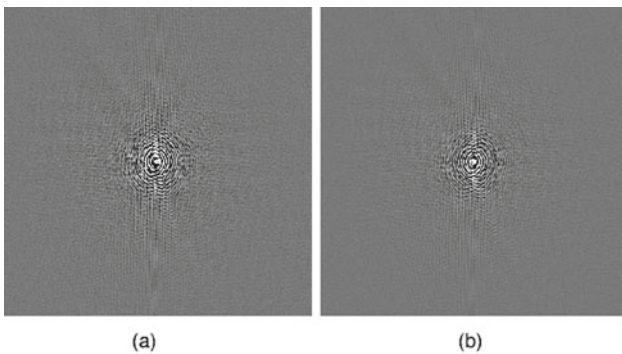


Fig. 12.7 The sine and cosine coefficients for the image in Fig. 12.6. **a** $C(k_x, k_y)$. **b** $S(k_x, k_y)$. Prepared by Mr. Tuong Huu Le, Center for Magnetic Resonance Research, University of Minnesota. Thanks also to Prof. Xiaoping Hu

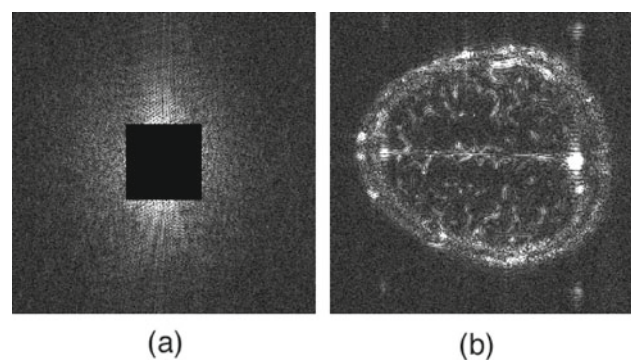


Fig. 12.10 The image that results when the low-frequency Fourier components below $k_{x \max}/4$ and $k_{y \max}/4$ are removed. Prepared by Mr. Tuong Huu Le, Center for Magnetic Resonance Research, University of Minnesota. Thanks also to Prof. Xiaoping Hu

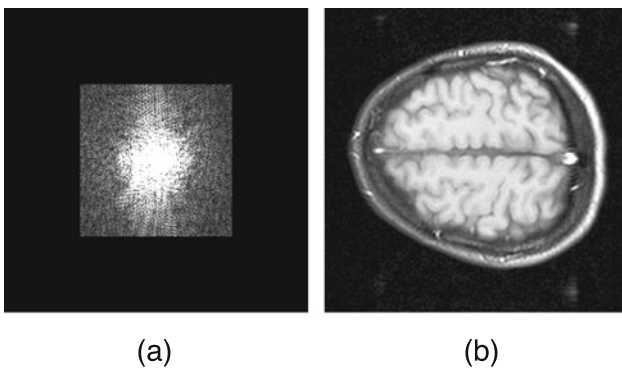


Fig. 12.8 The image that results when the high-frequency Fourier components above $k_{x \max}/2$ and $k_{y \max}/2$ are removed. Note the blurring compared to Fig. 12.6. Prepared by Mr. Tuong Huu Le, Center for Magnetic Resonance Research, University of Minnesota. Thanks also to Prof. Xiaoping Hu

they have been removed above $k_{x \max}/2$ and $k_{y \max}/2$. In the second they are removed above $k_{x \max}/4$ and $k_{y \max}/4$. Compare the blurring in these figures with the original image.

When the low-frequency coefficients are set to zero as in Fig. 12.10, only the high-frequency edges remain. In this case the Fourier components below $k_{x \max}/4$ and $k_{y \max}/4$ have been set to zero. (Keeping the same values of $k_{x \max}$ and Δk and removing the information on those coefficients keeps the field of view the same.)

Figure 12.11 shows the artifact that results from setting every other Fourier coefficient to zero: “ghost” images (Buonocore and Gao 1977). In the first case alternate Fourier coefficients have been removed in k_x space; in the second they have been removed in both k_x and k_y .

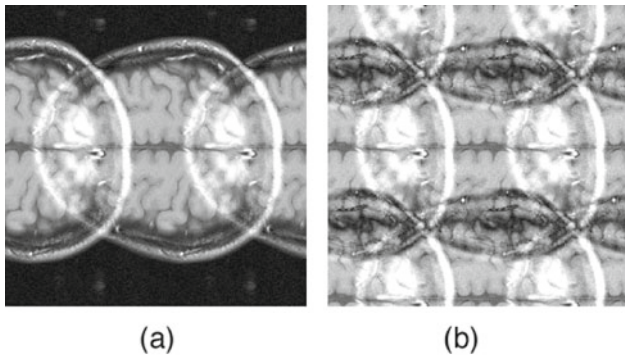


Fig. 12.11 The Fourier coefficients for every other value of k have been set to zero which leads to ghost images. **a** Every other value of k_x has been removed. **b** Every other value of both k_x and k_y has been removed. Prepared by Mr. Tuong Huu Le, Center for Magnetic Resonance Research, University of Minnesota. Thanks also to Prof. Xiaoping Hu

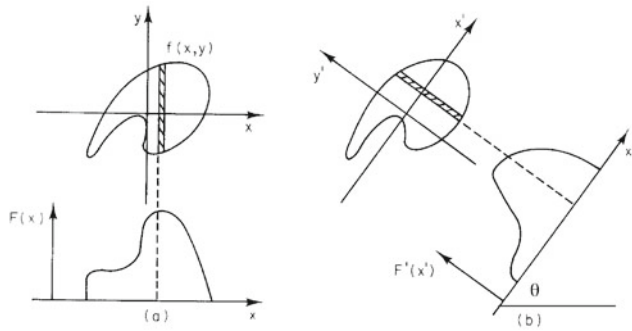


Fig. 12.12 **a** Function $F(x)$ is the integral of $f(x, y)$ over all y . **b** The scan is repeated at angle with the x axis

12.3.1 Summary

In summary: *The lowest spatial frequency in the image determines the field of view. The lower the minimum spatial frequency, the larger the field of view. Low spatial frequencies provide shape, contrast, and brightness.*

The highest spatial frequency in the image determines the resolution. The higher the maximum spatial frequency, the finer the resolution. High spatial frequencies provide resolution, edges, and sharp detail.

12.4 Two-Dimensional Image Reconstruction from Projections by Fourier Transform

The reconstruction problem can be stated as follows. A function $f(x, y)$ exists in two dimensions. Measurements are made that give *projections*: the integrals of $f(x, y)$ along various lines as a function of displacement perpendicular to each line. For example, integration parallel to the y axis gives

a function of x ,

$$F(x) = \int_{-\infty}^{\infty} f(x, y) dy, \tag{12.23}$$

as shown in Fig. 12.12. The scan is repeated at many different angles θ with the x axis, giving a set of functions $F(\theta, x')$, where x' is the distance along the axis at angle θ with the x axis. The problem is to reconstruct $f(x, y)$ from the set of functions $F(\theta, x')$. Several different techniques can be used. A detailed reference is the book by Cho et al. (1993).

We will consider two of these techniques: reconstruction by Fourier transform, where the Fourier coefficients are obtained from projections (in this section), and filtered back projection (Sect. 12.5).

The Fourier transform technique is easiest to understand. Consider Eqs. 12.9. If $k_y = 0$ in Eq. 12.9b, the result is

$$\begin{aligned} C(k_x, 0) &= \int_{-\infty}^{\infty} \cos(k_x x) dx \int_{-\infty}^{\infty} f(x, y) dy \\ &= \int_{-\infty}^{\infty} \cos(k_x x) F(\theta = 0, x) dx. \end{aligned} \tag{12.24}$$

Similarly

$$S(k_x, 0) = \int_{-\infty}^{\infty} \sin(k_x x) F(0, x) dx. \tag{12.25}$$

To state this in words: the Fourier transform of $F(0, x)$ determines the sine and cosine transforms of $f(x, y)$ along the line $k_y = 0$ (the k_x axis) in the spatial frequency plane. This is shown in Fig. 12.13.

A scan in another direction can be Fourier-transformed to give C and S at an angle θ with the k_x axis. The Fourier transform of the projection at angle θ is equal to the two-dimensional Fourier transform of the object, evaluated in the direction θ in Fourier transform space. This result is known as the *projection theorem* or the *central slice theorem* (Problem 20). The transforms of a set of projections at many different angles provide values of C and S throughout the $k_x k_y$ plane that can be used in Eq. 12.9a to calculate $f(x, y)$. In Chap. 18 we will find that the data from an MRI scan give the functions $C(k_x, k_y)$ and $S(k_x, k_y)$ directly.

In practice, the transforms are discrete. Using the notation that includes the redundant frequencies above $N/2$ and makes the coefficients half as large (Eqs. 11.27), the two-dimensional discrete Fourier transform (DFT) is²

$$f_{j k} = \sum_{l=0}^{N-1} \sum_{m=0}^{N-1} C_{l m} \cos \left[\frac{2\pi(j l + k m)}{N} \right] \tag{12.26a}$$

² In this notation the low frequencies occur for low values of the indices l and m . Usually, as in Figs. 12.6, 12.7, 12.8, 12.9, 12.10, and 12.11, the indices are shifted so $k = 0$ occurs in the middle of the sum.

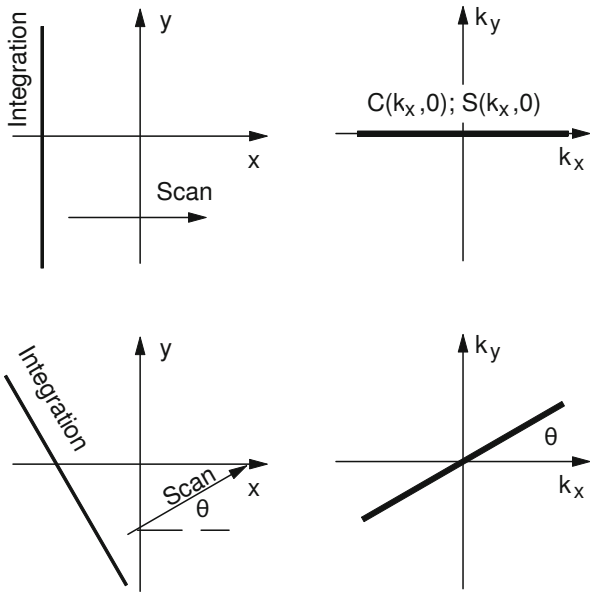


Fig. 12.13 The Fourier transform of $F(\theta = 0, x) = \int f(x, y)dy$ gives Fourier coefficients C and S along the k_x axis ($k_y = 0$). The Fourier transform of scans at other angles θ give C and S along corresponding lines in the $k_x k_y$ plane

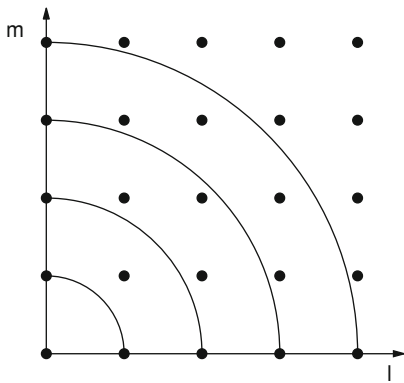


Fig. 12.14 The two-dimensional Fourier reconstruction requires values of C and S at the *lattice points* shown. The Fourier transforms of the projections $F(\theta, x)$ give the coefficients along the *circular arcs*. Interpolation is necessary to do the reconstruction

$$+ \sum_{l=0}^{N-1} \sum_{m=0}^{N-1} S_{lm} \sin \left[\frac{2\pi(jl + km)}{N} \right].$$

The coefficients are given by

$$C_{lm} = \frac{1}{N^2} \sum_{j=0}^{N-1} \sum_{k=0}^{N-1} f_{jk} \cos \left[\frac{2\pi(jl + km)}{N} \right], \quad (12.26b)$$

$$S_{lm} = \frac{1}{N^2} \sum_{j=0}^{N-1} \sum_{k=0}^{N-1} f_{jk} \sin \left[\frac{2\pi(jl + km)}{N} \right]. \quad (12.26c)$$

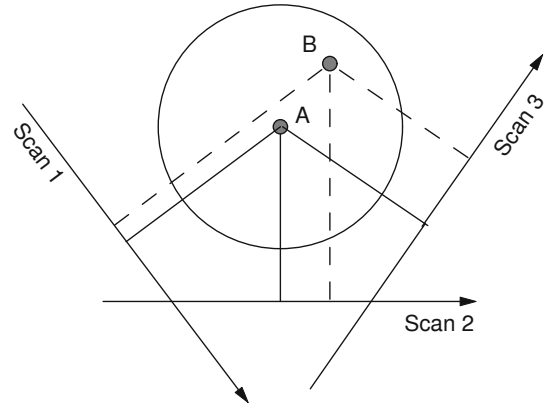


Fig. 12.15 The principle of back projection. Each point in the image is generated by summing all values of $F(\theta, x')$ that projected through that point. For point A at the center of rotation, the appropriate value of x' is the same at each angle. For other points such as B , the value of x' is different at each angle

Making a DFT of the projections gives values for C and S that lie on the circles in Fig. 12.14. But taking the inverse transform to calculate the reconstructed image requires values at the lattice points. They are obtained by interpolation (see Problem 23). The details of how the interpolation is made are crucial when using the Fourier transform reconstruction technique.

12.5 Reconstruction from Projections by Filtered Back Projection

Filtered back projection is more difficult to understand than the direct Fourier technique.³ It is easy to see that every point in the object contributes to some point in each projection. The converse is also true. In a back projection every point in each projection contributes to some point in the reconstructed image. This can be seen from Fig. 12.15, which shows two points A and B and three projections. For point A , which is at the center of rotation, the relevant value of x' is the same in each projection, while for point B the value of x' is different in each projection.

A very simple procedure would be to construct an image by back-projecting every projection. The back projection $f_b(x, y)$ at point (x, y) is the sum of $F(\theta, x')$ for every projection or scan, using the value of x' that corresponds to the original projection through that point. That is, for Fig. 12.15, the back projection at point A would be the sum of the three values for which the solid projection lines intersect the scans,

³ A simple experiment on back-projection using a laser pointer is described by Delaney and Rodriguez (2002).

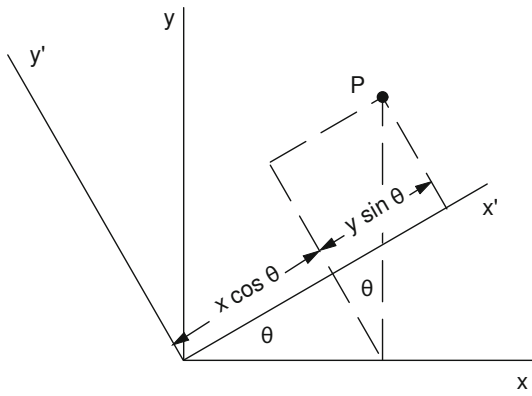


Fig. 12.16 By considering components of the coordinates of point P in both coordinate systems, one can derive the transformation equations, Eqs. 12.27 and 12.28

while for point B it would be the sum of the values where the three dashed lines strike the scans. This gives a rather crude image, but we will see how to refine it.⁴

Figure 12.16 shows how to relate the values of x' and y' for a projection at angle θ to the object or image coordinates x and y . The transformations are

$$\begin{aligned} x' &= x \cos \theta + y \sin \theta, \\ y' &= -x \sin \theta + y \cos \theta, \end{aligned} \tag{12.27}$$

and the inverse transformations are

$$\begin{aligned} x &= x' \cos \theta - y' \sin \theta, \\ y &= x' \sin \theta + y' \cos \theta. \end{aligned} \tag{12.28}$$

The projection at angle θ is integrated along the line y' :

$$\begin{aligned} F(\theta, x') &= \int f(x, y) dy' \\ &= \int f(x' \cos \theta - y' \sin \theta, x' \sin \theta + y' \cos \theta) dy'. \end{aligned} \tag{12.29}$$

The process of calculating $F(\theta, x')$ from $f(x, y)$ is sometimes called the *Radon transformation*. When $F(\theta, x')$ is plotted with x' on the horizontal axis, θ on the vertical axis, and F as the brightness or height on a third perpendicular axis, the resulting picture is called a *sinogram*. For example, the projection of $f(x, y) = \delta(x - x_0)\delta(y - y_0)$ is $F(\theta, x') = \delta(x' - (x_0 \cos \theta + y_0 \sin \theta))$. A plot of this object and its sinogram is shown in Fig. 12.17.

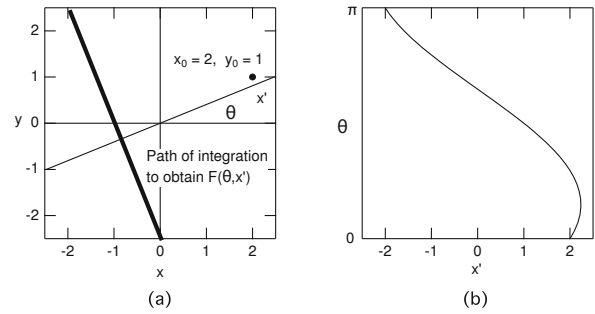


Fig. 12.17 An object and its sinogram. The object is a δ function at (x_0, y_0) . **a** The object and the path of a projection at angle θ . **b** A sinogram of the object $F(\theta, x')$. The value of F would be plotted on an axis perpendicular to the $x'\theta$ plane. The line shows the values of θ and x' for which F is nonzero

The definition of the back-projection is

$$f_b(x, y) = \int_0^\pi F(\theta, x') d\theta, \tag{12.30}$$

where x' is determined for each projection by using Eq. 12.27. The limits of integration are 0 and π since the projection for $\theta + \pi$ repeats the projection for angle θ .

We will now show that the image $f_b(x, y)$ obtained by taking projections of the object $F(\theta, x')$ and then back-projecting them is equivalent to taking the convolution of the object with the function $h(x - x', y - y') = 1/r$, where r is the distance in the xy plane from the object point to the image point. Function h depends only on the distance between the object and image points. This is discussed in greater detail by Barrett and Myers (2004, p. 280). To simplify the algebra, we find the back projection at the origin. We want the set of projections for $x' = 0$ as a function of scan angle θ . They are, from Eq. 12.29,

$$F(\theta, 0) = \int_{-\infty}^\infty f(-y' \sin \theta, y' \cos \theta) dy'. \tag{12.31}$$

In terms of angle $\theta' = \theta + \pi/2$ which is the angle from the x axis to the y' axis,

$$F(\theta', 0) = \int_{-\infty}^\infty f(y' \cos \theta', y' \sin \theta') dy'.$$

The arguments of f look very much like components of a vector, with magnitude r' and components $r' \cos \theta'$ and $r' \sin \theta'$. This suggests expressing the integral in polar coordinates. Since y' is a dummy variable, call it r' . In terms of r' and θ' the projection is

⁴ To see why it is crude, suppose the original object is a disk at the origin. Every projection will be the same because of the symmetry in angle. Every back projection will lay down a contribution to the

image along a stripe. Even though the reconstructed image will be largest where the original circle was, the image will have nonzero values throughout the image plane. We will see this example in Sect. 12.6.

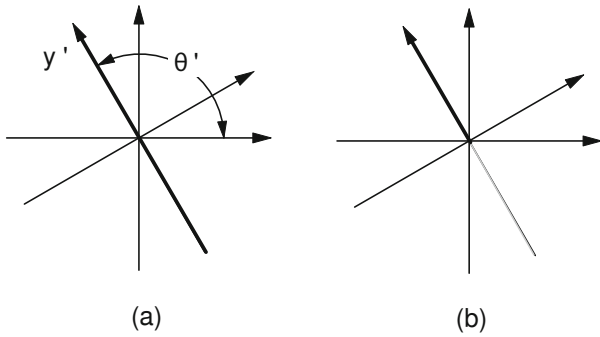


Fig. 12.18 Integration for the back projection is over y' from $-\infty$ to $+\infty$, as shown in **a**. This can be converted to an integral from 0 to ∞ if the angular integration is taken from 0 to 2π , as shown in **b**

$$F(\theta', 0) = \int_{-\infty}^{\infty} f(r', \theta') dr'. \quad (12.32)$$

Inserting this expression in Eq. 12.30 gives for the back projection

$$f_b(0, 0) = \int_0^{\pi} F(\theta', 0) d\theta' = \int_{-\infty}^{\infty} \int_0^{\pi} f(r', \theta') dr' d\theta'. \quad (12.33)$$

Figure 12.18a shows how y' (that is, r') is integrated from $-\infty$ to ∞ while θ' goes from 0 to π . For the purposes of Eq. 12.33 the limits of integration can be changed as in Fig. 12.18b. Variable r' can range from 0 to ∞ while θ' goes from 0 to 2π . Then the expression for f_b looks even more like an integration in polar coordinates:

$$f_b(0, 0) = \int_0^{\infty} \int_0^{2\pi} f(r', \theta') dr' d\theta'.$$

There is still one difference between this and polar coordinates. The element of area, which is $dx'dy'$ in Cartesian coordinates, is $r'dr'd\theta'$ in polar coordinates. Therefore, let us rewrite this as

$$f_b(0, 0) = \int_0^{\infty} \int_0^{2\pi} \left(\frac{f(r', \theta')}{r'} \right) r' dr' d\theta'. \quad (12.34)$$

We now change to the Cartesian variables x' and y' . The back-projected image at the origin is

$$f_b(0, 0) = \int_{-\infty}^{\infty} \int_{-\infty}^{\infty} \frac{f(x', y')}{(x'^2 + y'^2)^{1/2}} dx' dy'. \quad (12.35)$$

For an arbitrary point (x, y) the result is similar:

$$f_b(x, y) = \int_{-\infty}^{\infty} \int_{-\infty}^{\infty} \frac{f(x', y')}{[(x - x')^2 + (y - y')^2]^{1/2}} dx' dy'. \quad (12.36)$$

We have shown that the image obtained by taking projections of the object $F(\theta, x')$ and then back projecting them is equivalent to taking the convolution of the object with the function

$h(x - x', y - y') = 1/r$, where r is the distance in the xy plane from the object point to the image point.

The back-projected image is not a faithful reproduction of the object. But it is possible to manipulate the projections $F(\theta, x')$ to produce a function $G(\theta, x')$ whose back projection is the desired $f(x, y)$. This is the process of *filtering* before making the back projection. To find the relationship between F and the desired function G , note that there is some function $g(x, y)$ that we do not know, but which, when projected and then back projected, yields the desired function $f(x, y)$. That is,

$$f(x, y) = g_b(x, y) = \quad (12.37)$$

$$\int_{-\infty}^{\infty} \int_{-\infty}^{\infty} \frac{g(x', y')}{[(x - x')^2 + (y - y')^2]^{1/2}} dx' dy'.$$

Equations 12.10 relate the Fourier coefficients of f , g , and $h(r) = 1/r$:

$$C_f(k_x, k_y) = C_g(k_x, k_y)C_h(k_x, k_y) - S_g(k_x, k_y)S_h(k_x, k_y),$$

$$S_f(k_x, k_y) = C_g(k_x, k_y)S_h(k_x, k_y) + S_g(k_x, k_y)C_h(k_x, k_y).$$

These can be solved for

$$\begin{aligned} S_g &= \frac{C_h S_f - S_h C_f}{C_h^2 + S_h^2}, \\ C_g &= \frac{C_h C_f + S_h S_f}{C_h^2 + S_h^2}. \end{aligned} \quad (12.38)$$

One can show by direct integration (see Problem 31) that the Fourier transform of $h(r) = 1/r$ is

$$C_h(k_x, k_y) = 2\pi(k_x^2 + k_y^2)^{-1/2}, \quad (12.39)$$

$$S_h(k_x, k_y) = 0,$$

so that

$$C_g(k_x, k_y) = \frac{1}{2\pi}(k_x^2 + k_y^2)^{1/2}C_f(k_x, k_y), \quad (12.40)$$

$$S_g(k_x, k_y) = \frac{1}{2\pi}(k_x^2 + k_y^2)^{1/2}S_f(k_x, k_y).$$

If function $g(x, y)$ were known and were projected to give $G(\theta, x')$, then back-projecting G would give the desired $f(x, y)$. The final step is to relate $G(\theta, x')$ and $F(\theta, x')$ so that we do not have to know $g(x, y)$. To establish this relationship, consider a projection on the x axis. Equations 12.24 and 12.25 show that

$$\begin{aligned} F(0, x) &= \frac{1}{2\pi} \int_{-\infty}^{\infty} \\ & [C_f(k_x, 0) \cos(k_x x) + S_f(k_x, 0) \sin(k_x x)] dk_x, \end{aligned}$$

while

$$G(0, x) = \frac{1}{2\pi} \int_{-\infty}^{\infty} [C_g(k_x, 0) \cos(k_x x) + S_g(k_x, 0) \sin(k_x x)] dk_x.$$

Equations 12.40 relate the Fourier coefficients for F and G . For $k_y = 0$, $(k_x^2 + k_y^2)^{1/2} = |k_x|$. Therefore

$$G(0, x) = \left(\frac{1}{2\pi}\right)^2 \int_{-\infty}^{\infty} [C_f(k_x, 0) \cos(k_x x) + S_f(k_x, 0) \sin(k_x x)] |k_x| dk_x. \quad (12.41)$$

This result is independent of the choice of axis, so it must be true for any projection. There is a function $h(x)$ which can be convolved with any $F(\theta, x)$ to give the desired function $G(\theta, x)$. Equation 12.41 shows that

$$C_g(k_x, 0) = C_f(k_x, 0) |k_x| / 2\pi, \\ S_g(k_x, 0) = S_f(k_x, 0) |k_x| / 2\pi.$$

Comparison with Eqs. 12.9 shows that

$$C_h = |k_x| / 2\pi, \quad S_h = 0.$$

Therefore

$$h(x) = \left(\frac{1}{2\pi}\right)^2 \int_{-\infty}^{\infty} |k_x| \cos(k_x x) dk_x.$$

Because the integrand is an even function, we can multiply by 2 and integrate from zero to infinity. The integral to infinity does not exist. However, there is some maximum spatial frequency, roughly the reciprocal of the resolution we want, which we call $k_{x \max}$. We can therefore cut the integral off at this maximum spatial frequency and obtain

$$\begin{aligned} h(x) &= \frac{1}{2\pi^2} \int_0^{k_{x \max}} k_x \cos(k_x x) dk_x \\ &= \frac{1}{2\pi^2} \left[\frac{\cos(k_x x)}{x^2} + \frac{k_x \sin(k_x x)}{x} \right]_0^{k_{x \max}} \\ &= \frac{k_{x \max}^2}{(2\pi)^2} \left[2 \operatorname{sinc}(\xi) - \operatorname{sinc}^2(\xi/2) \right], \end{aligned} \quad (12.42)$$

where $\xi = k_{x \max} x$ and $\operatorname{sinc}(\xi) = \sin(\xi)/\xi$. The function $h(x)$ is plotted in Fig. 12.19. Using a sharp high-frequency cutoff introduces some problems, which are described below and which are easily overcome.

To summarize: *If each projection F is convolved with the function h of Eq. 12.42 and then back-projected, the back-projected image is equal to the desired image.*

Figure 12.20 summarizes the two methods of reconstructing an image from projections.

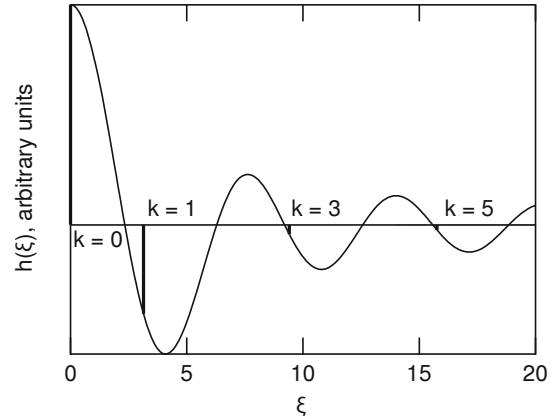


Fig. 12.19 The weighting function $h(x)$ of Eq. 12.42. The bars show the nonzero values for the example in Sect. 12.6

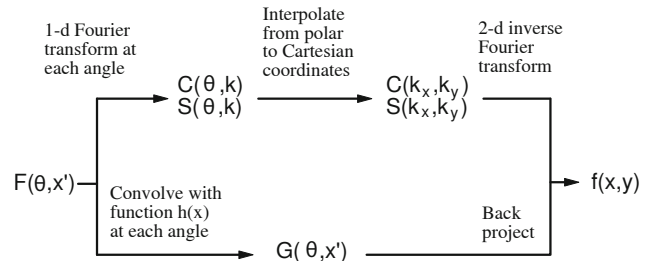


Fig. 12.20 A summary of the two methods for reconstructing an image

12.6 An Example of Filtered Back Projection

It is not difficult to write a computer program to perform filtered back projection if execution speed is not a concern. For our example we will use an object with circular symmetry, so that every projection is equivalent and only one projection needs to be convolved with the weighting function h . Because of the circular symmetry the back projection is needed only along one diameter. The program shown in Fig. 12.21 was used to reconstruct the image.

The “top-hat” function is used as the object:

$$f(x, y) = \begin{cases} 1, & x^2 + y^2 < a^2 \\ 0, & \text{otherwise.} \end{cases} \quad (12.43)$$

The projection is independent of θ : $F(x) = 2(a^2 - x^2)^{1/2}$ for $x^2 < a^2$. Procedure `CalCF` evaluates $F(x)$ for 100 points. Variables x and i are related by $x = 2i/N - 1$, so that x ranges from -1 to 1 as index i goes from 0 to 100. The value of a is 0.5.

The convolution is done by procedure `Convolve`, which uses convolving function h to operate on function F to produce G . The discrete form of h is obtained from Eq. 12.42 by the following argument, originally due to Ramachandran

```

// Circular Back Projection
#include <stdio.h>
#include <stdlib.h>
#include <math.h>
#define N 100 //Number of data points
const int n = N;
const double pi = 3.141592654;
double F[N], Image[N],
//Projection of object and image
// along a line [i]
G[N]; //Convolved Projection
void CalcF(double *F)
/*Calculates the projection of a
circle of radius a centered at N/2.*
{
    int i,i1,i2;
    double a = 0.5, x;
    i1 = (int)(50-a*((float)n)/2.0);
    i2 = (int)(50+a*((float)n)/2.0);
    for (i=0;i<n;i++)
    {
        x = 2*(i+1)/(float) n-1.0;
        F[i] = 0;
        if (i+1 > i1 && i+1 < i2)
            F[i] = F[i]+2*sqrt(pow(a,2)-
pow(x,2));}
    }
double H(int k)
{
    if (k==0)
        return pow((float)n,2)/16.0;
    else if(k%2 == 1 || (-k)%2 == 1)
        return -pow((float) n)/
        (pi*(float) k,2)/4.0;
    else
        return 0;
}
void Convolve(double*y, double*G)
{
    int i,j;
    double temp;
    for (i=0;i<n;i++)
    {
        temp = 0;
        for (j=0;j<n;j++)
            if (y[j] != 0)
                temp = temp+H(i-j)*y[j];
        G[i] = temp/((float) n);
    }
}
void BackProject(double*G,
double*Image)
{
    const int MaxProj = 180;
    int i,j,l;
    double x,xinterp,
        temp,c;
    for(i=0;i<n;i++)
        Image[i] = 0;
    for (j=0;j<MaxProj;j++)
        {
            c = cos(pi*((float) j)/180.0);
            for (i=0;i<n;i++)
                {
                    x = ((float)n)/2.0+(i+1
                    -((float) n)/2.0)*c;
                    l = (int) x;
                    xinterp = x-l;
                    if (l<=1)
                        temp = G[0];
                    else if(l>=n)
                        temp = G[n-1];
                    else
                        temp=G[l-1]+xinterp*(G[l]-G[l-1]);
                    Image[i] = Image[i]+temp;
                }
            }
        for(i=0;i<n;i++)
            Image[i] = Image[i]*pi/
            ((float) MaxProj);
    }
void PrintData(int n1, int n2,
double*x, FILE *fp, char *title)
{
    int i,j;
    fprintf(fp, "\n\n%s\n",title);
    j = 0;
    for (i = n1 -1; i < n2; i++)
        {
            if (j%10 == 0)
                fprintf(fp, "\n%2i",i+1);
            fprintf(fp, "\t%8.3f",x[i]);
            j++;
        }
    fprintf(fp, "\t%8.3f",x[i]);
}
void main()
{
    FILE *ofp;
    if (!(ofp =
fopen("OutputFile", "w")))
        {
            printf("cannot open output
file\n");
            exit(1);
        }
    fprintf(ofp, "\n");
    CalcF(F);
    PrintData(1,n,F,ofp, "Projected
Object
F");
    Convolve(F,G);
    PrintData(1,n,G,ofp, "Convolved
Projection G");
    BackProject(G,Image);
    PrintData(1,n,Image,ofp, "Back-
Projected
Image");
    fclose(ofp);
}

```

Fig. 12.21 The program used to make a filtered back projection of a circularly symmetric function

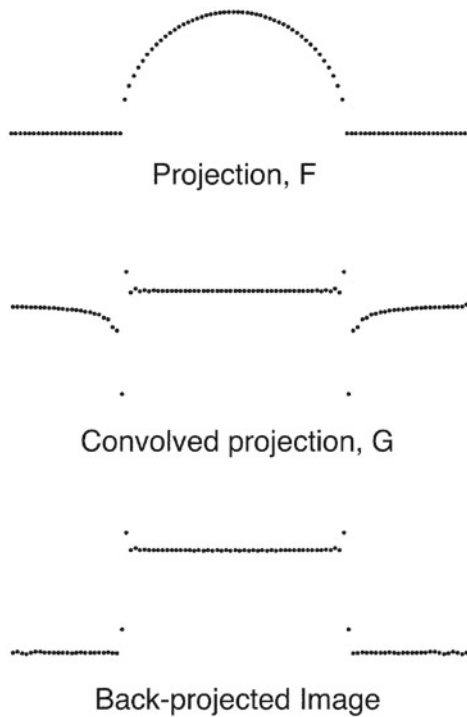


Fig. 12.22 Reconstruction of a circularly symmetric image by filtered back projection. **a** The projection $F(x)$. **b** The convolved projection $G(x)$. **c** The image from back-projecting the convolved data

and Lakshminarayanan (see Cho et al. 1993, p. 80). Variable x is considered on the interval $(-1, 1)$, so the period is 2 and $\omega_0 = \pi$. The maximum spatial frequency is $k_{x \max} = N\pi/2$. The value of x in the weighting function $h(x)$ depends on the value of index $k = i - j$: $x_i - x_j = 2(i - j)/N = 2k/N$. Therefore $\xi = k_{x \max}x = (N\pi/2)(2/N)k = \pi k$, where k is an integer. From Eq. 12.42 we obtain

$$h(k) = \begin{cases} N^2/16, & k = 0 \\ 0, & k \text{ even} \\ -N^2/4k^2\pi^2 & k \text{ odd.} \end{cases} \quad (12.44)$$

Procedure `Convolve` replaces the integral of Eq. 12.4a by a sum. The factor dx in the integral becomes $1/N$ in the sum.

Procedure `BackProject` forms the image from G . One hundred eighty projections are done in 1° increments from 0 to 179. The value of x is determined from $x = i \cos \theta$, but it is shifted so that the rotation takes place about $i = 50$. Unless x is at the end points, the value of G is obtained by linear interpolation. The value of $\Delta\theta$ used to convert the integral to a sum is $\pi/180$.

Procedure `PrintData` writes the data for the plots shown in Fig. 12.22. One can see from inspection of Fig. 12.22 how the convolution converts the semicircular projection F into a function G that is flat-topped over the



Fig. 12.23 Reconstruction by simple back projection without convolution. The object is the same as in Fig. 12.22

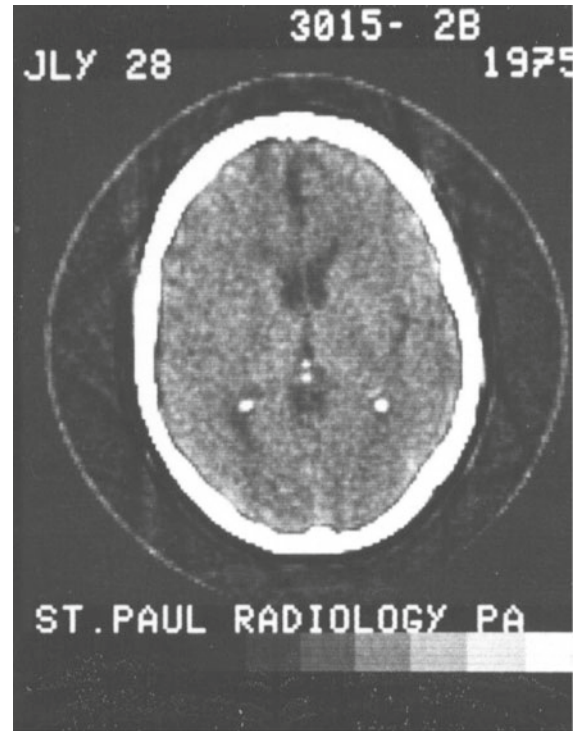


Fig. 12.24 An early CT brain scan, showing ringing inside the skull. Photograph courtesy of St. Paul Radiology Associates, St. Paul, MN

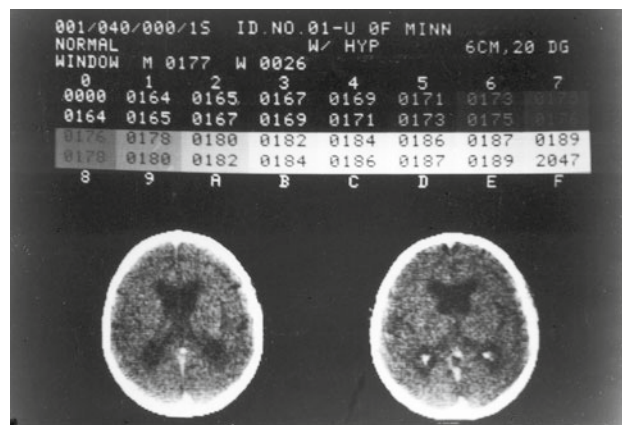


Fig. 12.25 Brain scans using a gradual high-frequency cutoff to eliminate ringing. Photograph courtesy of Prof. J. T. Payne, Department of Diagnostic Radiology, University of Minnesota

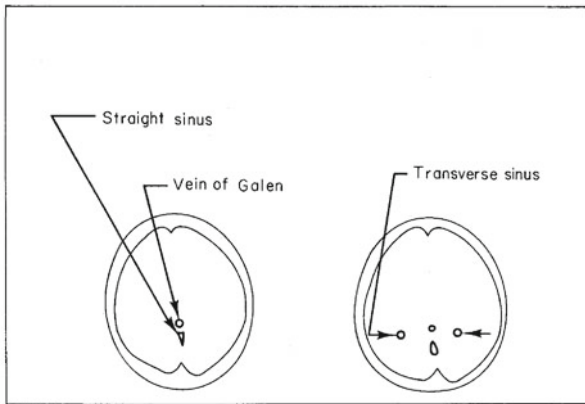


Fig. 12.26 Anatomic features shown in Fig. 12.25

region of nonvanishing f and has a negative contribution in the wings. Figure 12.23 shows what the image looks like if the back projection is done without first performing the convolution.

One can also see from Fig. 12.22 that ringing is introduced at the sharp edges. This is characteristic of the sharp high-frequency cutoff at k_x (similar to the Fourier series representation of a square wave with only a finite number of terms). Early computer tomography (CT) scans created with the convolution function presented here showed a dark band just inside the skull where there was an abrupt change in $f(x, y)$ upon going from bone to brain (Fig. 12.24). A gradual high-frequency cutoff changes the details of $h(k)$ and eliminates this ringing (Fig. 12.25). Fig. 12.26 shows the anatomic details of Fig. 12.25.

Symbols Used in Chap. 12

Symbol	Use	Units	First used page
a, b	Constants		348
a	Radius of “top-hat” function	m	355
b'	Length of object	m	346
f, g	Arbitrary functions		345
f_b, g_b	Back-projected images of f, g		353
h	Point spread function; impulse response for convolution		345
i	$\sqrt{-1}$		347
j, k	Subscript indices for data		352
k, k_x, k_y	Spatial frequencies	m^{-1}	346
l, m	Subscript indices for Fourier coefficients		351
m	Magnification		347
t, t'	Time or arbitrary variable		345

x, y, x', y'	Distance; coordinates in image or object plane; rotated coordinate system for image reconstruction	m	346
A	Amplitude		346
C_f	Fourier cosine transform of function f		346
D	Length of image	m	349
E	Function describing an image		347
F	Projection of function f		351
F, G, H	Complex Fourier transforms of f, g, h		347
L	Property describing an object		347
L	Width of image or Field of View (FOV)	m	349
N	Total number of data points; number of discrete values in one dimension of an image		349
S_f	Fourier sine transform of function f		346
T	Period	s	346
$\delta(t)$	Dirac delta function	s^{-1}	345
λ	Wavelength	m	346
ϕ	Phase		346
θ, θ'	Angle		351
τ_1	Time constant	s	346
ω, ω_0	Angular frequency	(radian) s^{-1}	346
ξ	Dummy variable		353

Problems

Section 12.1

Problem 1. Compare Eq. 12.4a to Eqs. 4.73 and 7.21 and deduce the impulse response for those two systems.

Problem 2. Except for the minus sign, Eq. 12.4a is the same integral that defines the cross-correlation function. There are some important differences, however. Show that the convolution function is commutative—interchanging the order of variables gives the same result—but that the cross-correlation function is not.

Problem 3. (a) Use the convolution integral, Eq. 12.4a, to calculate the convolution $g(t)$ of the function $h(t - t')$ in Eq. 12.5 with

$$f(t) = \begin{cases} 1, & 0 < t < T, \\ 0, & \text{otherwise} \end{cases}$$

Plot $f(t)$ and $g(t)$.

(b) Calculate the Fourier transform of $g(t)$, $h(t - t')$, and $f(t)$ from part (a), and show that they obey Eq. 12.6a.

Problem 4. Fill in the details in the derivation of Eq. 12.6a.

Problem 5. Use the convolution integral to calculate $g(x)$ from $h(x - x') = a/[a^2 + (x - x')^2]$ and $f(x) = \cos(kx)$.

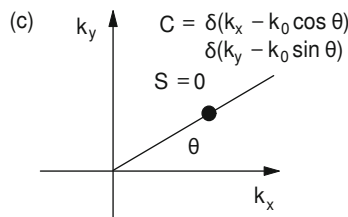
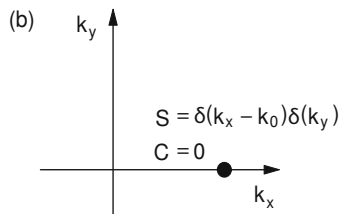
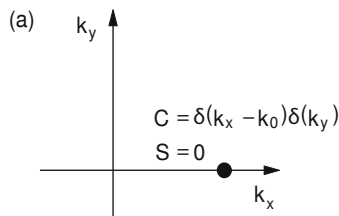
Interpret this physically as a spatial frequency filter. Hint:

$$\int_{-\infty}^{\infty} \frac{\cos(ky)dy}{y^2 + b^2} = \frac{\pi}{b} e^{-kb},$$

$$\int_{-\infty}^{\infty} \frac{\sin(ky)dy}{y^2 + b^2} = 0.$$

Problem 6. If you are familiar with complex variables, use the definition of the Fourier transform in Eq. 12.11a to prove the convolution theorem, Eq. 12.11b.

Problem 7. What are the two-dimensional images whose Fourier transforms are shown?



Problem 8. Calculate the two-dimensional Fourier transform of the function

$$f(x, y) = \begin{cases} 1, & -a/2 < x < a/2, \quad -b/2 < y < b/2, \\ 0, & \text{otherwise.} \end{cases}$$

Plot $f(x, y)$ vs x and y and $C_f(k_x, k_y)$ vs k_x and k_y for $a = 2b$.

Problem 9. Calculate the two-dimensional Fourier transform of the function

$$f(x, y) = \operatorname{sech}\left(\frac{x}{a}\right) \operatorname{sech}\left(\frac{y}{b}\right).$$

You may need the relationship

$$\int_0^{\infty} \operatorname{sech}(uz) \cos(vz)dz = \frac{\pi}{2u} \operatorname{sech}\left(\frac{\pi v}{2u}\right).$$

Problem 10. Calculate the two-dimensional Fourier transform of the function

$$f(x, y) = \begin{cases} 1, & \sqrt{x^2 + y^2} < a, \\ 0, & \sqrt{x^2 + y^2} > a. \end{cases}$$

Hint: convert to polar coordinates in both the xy and $k_x k_y$ planes, and use the facts that

$$J_0(u) = \frac{1}{2\pi} \int_0^{2\pi} \cos(u \cos v)dv,$$

$$\int u J_0(u)du = u J_1(u),$$

where J_0 and J_1 are Bessel functions of order zero and order one. Bessel functions are tabulated and have known properties, similar to trigonometric functions. See Abramowitz and Stegun (1972), p. 360.

Section 12.2

Problem 11. Complete the verification of Eq. 12.13 suggested in the text.

Problem 12. Find the Fourier transform of the point spread function for the ideal imaging system, Eq. 12.13.

Problem 13. Use Eq. 12.15 to show that the sum of the squares of the Fourier coefficients of the image is equal to the sum of the squares of the Fourier coefficients of the object times the square of the modulation transfer function, for a given set of spatial frequencies (k_x, k_y) .

Problem 14. Write the modulation of the image in terms of the variables in Eq. 12.19.

Problem 15. How does magnification m change the spatial frequencies in going from object to image? Since one is concerned about seeing detail in the object, resolution and spatial frequencies are usually converted to object coordinates in medical imaging, while they are left in terms of the detector coordinates in photography.

Section 12.3

Problem 16. This problem shows how increasing the detail in an image introduces high-frequency components. Find the continuous Fourier transform of the two functions

$$f_1(x) = \begin{cases} 0, & x < 0, \\ 1, & 0 < x < 1, \\ 0, & x > 1 \end{cases}$$

$$f_2(x) = \begin{cases} 0, & x < 0, \\ \sqrt{3/2}, & 0 < x < 1/3, \\ 0, & 1/3 < x < 2/3, \\ \sqrt{3/2}, & 2/3 < x < 1, \\ 0, & x > 1. \end{cases}$$

Plot $a(k_x) = [C^2(k_x) + S^2(k_x)]^{1/2}$ for each function using a spreadsheet or plotting package, for the range $-45 < k_x < 45$. Compare the features of each plot. Both functions have the same value of $\int_{-\infty}^{\infty} f^2(x) dx$.

Problem 17. To see the blurring effect shown in Fig. 12.8 consider a one-dimensional problem. Let $y_0 = 1$ and $y_j = 0$ for $j = 1, 2, \dots, 7$. Use Eqs. 11.27b and 11.27c to calculate the discrete Fourier transform of this function a_k and b_k for $k = 0, 1, 2, \dots, 7$. Then remove the high frequencies by setting $a_k = b_k = 0$ for $k = 2, 3, 4, \dots, 6$, as was done in Fig. 12.8. (Note that the $k = 7$ point is equivalent to $k = -1$ and therefore acts like a “low” frequency.) Use Eq. 11.27a to calculate new values of y_j . Do you get a blurred image?

Problem 18. To see the edge effect in Fig. 12.10, consider the one-dimensional function defined in Problem 17. After calculating the discrete Fourier transform a_k and b_k , remove the low frequencies by setting $a_k = b_k = 0$ for all k except $k = 3, 4, 5$ as was done in Fig. 12.10. (Note that the points $k = 6$ and 7 are equivalent to $k = -2$ and $k = -1$ and therefore act like “low” frequencies.) Use Eq. 11.27a to calculate new values of y_j . Do you get an image with edge effects?

Problem 19. To see the ghost image effect in Fig. 12.11, consider the one-dimensional function described in Problem 17. After calculating the discrete Fourier transform a_k and b_k , set $a_k = b_k = 0$ for all odd values of k as was done in Fig. 12.11. Use Eq. 11.27a to calculate new values of y_j . Do you get a “ghost image?”

Section 12.4

Problem 20. Prove the central slice theorem analytically. Consider the cosine term of the 2-dimensional Fourier transform $C(k_x, k_y)$ in Eq. 12.9b. Rotate to the primed coordinates given by Eq. 12.28. Note that the area element $dx dy$ transforms to $dx' dy'$. Express C as a function of polar coordinates in k -space, $k_x = k \cos \theta$ and $k_y = k \sin \theta$. Show that

$$C(\theta, k) = \int_{-\infty}^{\infty} F(\theta, x') \cos(kx') dx',$$

$$S(\theta, k) = \int_{-\infty}^{\infty} F(\theta, x') \sin(kx') dx'.$$

Problem 21. Suppose that $f(x, y)$ is independent of y . Find expressions for $C(k_x, k_y)$ and $S(k_x, k_y)$ and insert them in

the expression for $f(x, y)$ to verify that $f(x, y)$ is recovered. You will need Eqs. 11.66.

Problem 22. Suppose that the object is a point at the origin, so that $f(x, y) = \delta(x)\delta(y)$. Find the projection $F(x)$ and the transform functions $C(k_x, 0)$ and $S(k_x, 0)$. Use these results to reconstruct the image using the Fourier technique.

Problem 23. Figure 12.14 shows that taking the Fourier transform of the projection $F(\theta, x')$ gives the Fourier coefficients $C(k, \theta)$ at points along circular arcs in frequency space. In order to get these coefficients at equally spaced points in x and y , interpolation is necessary. One simple method is to use *bilinear interpolation* (Press et al. 1992). Suppose you know the Fourier coefficients at points $r_i = i \Delta r$, $\theta_j = j \Delta \theta$, and you want to get the Fourier coefficients at points $x_n = n \Delta x$, $y_m = m \Delta y$. For a given x_n, y_m , convert to polar coordinates to get r and θ , then find the four known points that “surround” the desired point. The value of the coefficient is

$$C(x_n, y_m) = \frac{1}{\Delta r \Delta \theta} [C(r_i, \theta_j)(r_{i+1} - r)(\theta_{j+1} - \theta) + C(r_{i+1}, \theta_j)(r - r_i)(\theta_{j+1} - \theta) + C(r_i, \theta_{j+1})(r_{i+1} - r)(\theta - \theta_j) + C(r_{i+1}, \theta_{j+1})(r - r_i)(\theta - \theta_j)].$$

Suppose $C(r, \theta) = \sin(r)/r$, which is also called $\text{sinc}(r)$. If C is known at points with $\Delta r = 0.5$ and $\Delta \theta = \pi/8$, evaluate C at point $x = 2, y = 3$ using bilinear interpolation. Compare this result to the exact value of $C = \text{sinc}((x^2 + y^2)^{1/2})$. Try this for other points (x_n, y_m) .

Section 12.5

Problem 24. Derive Eqs. 12.27 and 12.28.

Problem 25. An object is described by the function $f(x, y) = e^{-(x^2+y^2)/b^2}$.

(a) Find the Fourier transform $C(k_x, k_y)$ and $S(k_x, k_y)$ directly from Eqs. 12.9 b and c.

(b) Find the projection $F(\theta, x')$ using Eq. 12.29. Then take the 1-dimensional Fourier transform of $F(\theta, x')$ using the equations

$$C(\theta, k) = \int_{-\infty}^{\infty} F(\theta, x') \cos kx' dx'$$

$$S(\theta, k) = \int_{-\infty}^{\infty} F(\theta, x') \sin kx' dx'.$$

Use $k = (k_x^2 + k_y^2)^{1/2}$ to express C and S in terms of k_x and k_y . Your answer should be the same as part (a).

Use the following integral table:

$$\int_{-\infty}^{\infty} e^{-az^2} dz = \sqrt{\frac{\pi}{a}}$$

$$\int_{-\infty}^{\infty} e^{-az^2} \cos bz dz = \sqrt{\frac{\pi}{a}} e^{-b^2/4a}$$

$$\int_{-\infty}^{\infty} e^{-az^2} \sin bz dz = 0.$$

Problem 26. Assume you have just measured the projection function $F(\theta, x') = \pi^{1/2} b e^{-(x'-a \cos \theta)^2/b^2}$. (For this problem, ignore the fact that your measuring device would only give F at discrete values of θ and x' .)

- (a) Find $f(x, y)$ using the Fourier method. You may need the integrals from Problem 25.
- (b) Qualitatively sketch plots of the object $f(x, y)$ and the sinogram $F(\theta, x')$. Use a gray scale to indicate the magnitude of f and F .

Problem 27. Repeat Problem 26 using

$$F(\theta, x') = \frac{a\sqrt{\pi}}{2} e^{-x'^2/a^2} \left[1 + \cos^2 \theta \left(2 \frac{x'^2}{a^2} - 1 \right) \right].$$

Look up any integrals you need.

Problem 28. Suppose an object is a point at the origin, $f(x, y) = \delta(x)\delta(y)$. The projection is also a point: $F(\theta, x') = \delta(x')$. Calculate the back projection $f_b(x, y)$ (without filtering) using Eq. 12.30. To solve the problem, use this property of δ functions:

$$\delta(g(u)) = \sum_i \frac{\delta(u - u_i)}{|dg/du|_{u=u_i}},$$

where the u_i are the points such that $g(u_i) = 0$. Note that the back projection is not a point. Back projection without filtering does not recover the object.

Problem 29. This problem is an extension of Problem 28, but the object is no longer at the origin. Let $f(x, y) = \delta(x - x_0)\delta(y - y_0)$.

- (a) Calculate $F(\theta, x')$. You may need the following properties of the δ function: $\int \delta(b - z)\delta(z - a)dz = \delta(b - a)$, $\delta(az) = \delta(z)/|a|$.
- (b) Use the function $F(\theta, x')$ you found in part (a) to calculate the back projection $f_b(x, y)$ using Eq. 12.30. You will need the property of the δ function given in Problem 28.
- (c) Show that $f_b(x, y)$ is equivalent to the convolution of $f(x, y)$ with the function $1/\sqrt{(x - x')^2 + (y - y')^2}$.

Problem 30. Here is an easy way to show that the back projection $f_b(x, y)$ cannot be equivalent to the object $f(x, y)$. If $f(x, y)$ is dimensionless, determine the units of $F(\theta, x')$ and $f_b(x, y)$. Do $f(x, y)$ and $f_b(x, y)$ have the same units?

Problem 31. Consider the Fourier transform of $1/r$. The coefficients are given by

$$C(k_x, k_y) = \int_{-\infty}^{\infty} \int_{-\infty}^{\infty} \frac{dx dy \cos(k_x x + k_y y)}{(x^2 + y^2)^{1/2}},$$

$$S(k_x, k_y) = \int_{-\infty}^{\infty} \int_{-\infty}^{\infty} \frac{dx dy \sin(k_x x + k_y y)}{(x^2 + y^2)^{1/2}}.$$

Transform to polar coordinates ($x = r \cos \theta, y = r \sin \theta$). Show from symmetry considerations of the angular integral that $S = 0$. Use the facts about the Bessel functions in Problem 10 and

$$\int_0^{\infty} J_0(kr) dr = 1/k$$

to derive Eqs. 12.39. The function $J_0(x)$ is a *Bessel function of order zero*. It is tabulated and has known properties, similar to a trigonometric function. See Abramowitz and Stegun (1972, p. 360).

Problem 32. An object consists of three δ functions at $(0, 2)$, $(\sqrt{3}, -1)$, and $(-\sqrt{3}, -1)$. Draw the sinogram of the object.

Problem 33. Let $f(x, y) = 1/[(x - a)^2 + y^2 + b^2]$. Calculate $F(\theta, x')$. Qualitatively sketch plots of the object $f(x, y)$ and the sinogram $F(\theta, x')$. Use a gray scale to indicate the magnitude of f and F .

Problem 34. Let $f(x, y) = x/(x^2 + y^2)^2$. Calculate $F(\theta, x')$. Qualitatively sketch plots of the object $f(x, y)$ and the sinogram $F(\theta, x')$. Use a gray scale to indicate the magnitude of f and F . Hint:

$$\int \frac{du}{(u^2 + v^2)^2} = \frac{u}{2v^2(u^2 + v^2)} + \frac{1}{2|v|^3} \tan^{-1} \left(\frac{u}{v} \right).$$

Problem 35. Consider the object $f(x, y) = a/\sqrt{a^2 - x^2 - y^2}$ for $\sqrt{x^2 + y^2} < a$, and 0 otherwise.

- (a) Plot $f(x, 0)$ vs x .
- (b) Calculate the projection $F(\theta, x')$. Plot $F(0, x')$ vs x' .
- (c) Use the projection from part (b) to calculate the back projection $f_b(x, y)$. Plot $f_b(x, 0)$ vs x .
- (d) Compare the object and the back projection. Explain qualitatively how they differ.

Section 12.6

Problem 36. Verify that

$$F(\theta, x) = \begin{cases} 2\sqrt{a^2 - x^2}, & |x| < a \\ 0, & |x| > a \end{cases}$$

is the projection of the function in Eq. 12.43.

Problem 37. Verify Eqs. 12.44.

Problem 38. Modify the program of Fig. 12.21 and run it without the convolution.

Problem 39. Modify the program of Fig. 12.21 to reconstruct an annulus instead of a top-hat function.

References

- Abramowitz M, Stegun IA (1972) Handbook of mathematical functions with formulas, graphs and mathematical tables. Government Printing Office, Washington, DC
- Barrett HH, Myers KJ (2004) Foundations of image science. Wiley-Interscience, New York
- Buonocore MH, Gao L (1977) Ghost artifact reduction for echo planar imaging using image phase correction. *Magn Reson Med* 38: 89–100.
- Cho Z-h, Jones JP, Singh M (1993) Foundations of Medical Imaging. Wiley, New York
- Delaney C, Rodriguez J (2002) A simple medical physics experiment based on a laser pointer. *Am J Phys* 70(10):1068–1070
- Gaskill JD (1978) Linear systems, fourier transforms, and optics. Wiley, New York
- Kevles BH (1997) Naked to the bone: medical imaging in the twentieth century. Rutgers University Press, New Brunswick
- Press WH, Teukolsky SA, Vetterling WT, Flannery BP (1992) Numerical recipes in C: the art of scientific computing. 2nd ed. reprinted with corrections, 1995. Cambridge University Press, New York
- Ramachandran GN, Lakshminarayanan AV (1971) Three-dimensional reconstruction from radiographs and electron micrographs: application of convolutions instead of Fourier transforms. *Proc Nat Acad Sci USA* 68:2236–2240
- Shaw R (1979). Applied optics and optical engineering. Academic, New York, pp 121–154. (Photographic Detectors. Ch. 5 Vol. 7).
- Williams CS, Becklund OA (1972) Optics: a short course for engineers and scientists. Wiley, New York